RESEARCH ARTICLE

A statistical method for transforming temporal correlation functions from one-point measurements into longitudinal spatial and spatio-temporal correlation functions

H. Nobach · C. Tropea

Abstract The transformation of temporal, one-point correlation functions into longitudinal spatial and spatio-temporal correlation functions in turbulent flows using a simple statistical convection model is introduced. To illustrate and verify the procedure, experimental data (one-point and two-point) have been obtained with a laser Doppler system from a turbulent, round, free-air jet.

1 Introduction

In the study of turbulence, temporal and spatial correlation functions are fundamental quantities defining characteristic scales of motion. In particular, integral scales and Taylor microscales are directly defined from the correlation function and, under the hypothesis of local isotropy, an estimate of the rate of dissipation per unit mass can be obtained.

Experimentally, measurements of correlation functions have often been performed using single-point measurement techniques, for example with stationary hot-wire probes (e.g., Favre 1965) or laser Doppler anemometers (e.g., Romano et al. 1999). Temporal Eulerian correlation functions can be obtained directly from the measured time series. Two-point or spatial correlation functions can be

H. Nobach (✉)
Max Planck Institute for Dynamics and Self-Organization,
Am Faßberg 17, 37077 Göttingen, Germany
e-mail: holger.nobach@nambis.de

C. Tropea
Center of Smart Interfaces, Institute of Fluid Mechanics and
Aerodynamics, Technische Universität Darmstadt,
Petersenstr. 30, 64287 Darmstadt, Germany
e-mail: ctropea@sla.tu-darmstadt.de

obtained with an array of multiple probes or, sequentially, with two measurement probes at varied separations. With particle image velocimetry (PIV), the Eulerian spatial correlation can be measured directly from the spatially resolved velocities at given time instances. However, the temporal and spatial resolution of PIV usually lacks the requirements to obtain small scales, for example the Taylor microscale, with sufficient accuracy. High-speed particle tracking (e.g., Ouellette et al. 2006) allows the Lagrangian correlation statistics to be obtained.

Without spatially resolved data, longitudinal two-point or spatial correlation functions are often approximated by using single-point, temporal correlation functions and invoking Taylor's frozen flow hypothesis (Taylor 1938) (TH), which assumes that the fluctuating velocity u' is small compared to the mean velocity U, that is, $u'/U \ll 1$, thus, spatially fluctuating quantities of the advected fluid along a path line of the fluid can be observed as temporal fluctuations at a given point. The functions investigated in the past span from local derivatives of velocities or of passive scalars like the temperature, where TH reads

$$\frac{\partial}{\partial t} = -U \frac{\partial}{\partial x},$$

to statistical functions f, like correlations or structure functions, using

$$f(x + \xi, t) = f(x, t - \xi/U).$$

or

$$f(x, t + \tau) = f(x - U\tau, t)$$

Although TH requires small fluctuations compared with the mean advective velocity, it has not seldom been applied to turbulent flows, where the above condition is no longer met. Here, as expected, it has been observed that TH works

well only at small scales, smaller than the typical scale of the flow (Lin 1953), where local homogeneity can be assumed. Corrections due to the fluctuating advective velocity may or may not be necessary (Heskestad 1965; Tennekes 1975; Browne et al. 1983; Hill 1996).

If applied to functions on larger scales, corrections of the TH become necessary, considering the variations of the velocity in a turbulent flow. Cholemari and Arakeri (2006) introduce methods which give a correspondence between the temporal and longitudinal spatial correlations by translating the time lag into separation or vice versa. However, they cannot be used to derive the spatio-temporal correlations, which decrease in amplitude for larger separations. Cenedese et al. (1991) predict the decrease in correlation by transfer functions, which work as a phase shifter from lower to higher frequencies. In He and Zhang (2006) and Zhao and He (2009), an elliptical approximation based on the second-order Taylor-series expansion of the spatio-temporal correlation function is introduced, reproducing well the shift and deformation of the correlation peak. However, the latter two methods describe the effect phenomenologically and require empirical parameters to be adapted to the measured data.

In the present study, an integral method based on the probability density distribution of the fluid velocity is proposed to transform temporal into longitudinal spatial and spatio-temporal correlation functions (Sect. 2). The procedure is validated by comparing results to two-point correlations measured directly with a laser Doppler system from a turbulent, round, free-air jet (Sect. 3).

2 Integral time-to-length transform

To transform a temporal correlation function into a longitudinal spatial correlation function, the spatio-temporal correlation function

$$R(\xi, \tau) = \langle u'(x,t)u'(x+\xi, t+\tau) \rangle$$

is introduced, where the chevrons mean the expectation of the inner term. The temporal correlation function obtained from single-point measurements then is $R(0, \tau)$ with the time delay τ and no separation ($\xi = 0$). The transformation into the longitudinal spatial correlation function with the separation ξ and no time delay is then

$$R(\xi, 0) = R(0, -\theta) \tag{1}$$

with the time of flight θ, which the flow needs to cover the separation ξ. Allowing both arguments, ξ and τ of the transformed correlation function to be varied, the spatio-temporal correlation function

$$R(\xi, \tau) = R(0, \tau - \theta) \tag{2}$$

is obtained.

TH assumes that the flow is "frozen" while it moves through the measurement point(s) with the mean velocity U yielding

$$\theta = \frac{\xi}{U} \tag{3}$$

Turbulent flows with fluctuating velocity $u(t)$ may significantly differ from this "frozen" hypothesis. The idea of the new integral time-to-length transform (ITLT) is that any fluid structure with a specific temporal correlation function, which has been measured at a specific point, can move to another point in flow direction within a certain time. This time depends on the varying fluid velocity u. While TH assumes that this velocity is constant, namely the mean velocity U, ITLT considers that the velocity and also the time to cover the separation between the two points can vary.

For a given separation ξ, every possible velocity value u yields a different time of flight θ. For given ξ and u, the time of flight is determined by

$$\theta = \frac{\xi}{u} \tag{4}$$

assuming that u does not change within the separation ξ (or within the time of flight θ). If u has a probability density function $p_u(u)$, then (for a given ξ) the time of flight has a probability density of

$$p_\theta(\theta) = \frac{|\xi|}{\theta^2} p_u(\xi/\theta) \tag{5}$$

Integration over all possible times of flight yields an averaged spatio-temporal correlation function

$$R(\xi, \tau) = \int_{-\infty}^{\infty} R(0, \tau - \theta) p_\theta(\theta) \, \mathrm{d}\theta \tag{6}$$

3 Experimental verification

Laser Doppler data have been taken in a turbulent, round, free-air jet, as illustrated in Fig. 1. The flowfield consists of the turbulent inner jet and an outer co-flow. Both parts of the flowfield are seeded. The co-flow is slow and has a low turbulence intensity of about 1 %. The velocity of the outer co-flow is expected to be uniform over the outlet, while the velocity profile of the inner flow is fully developed. The flow specifications are summarized in Table 1 and the specifications of the laser Doppler system in Table 2. A two-velocity component laser Doppler system has been used with two independent probes, yielding a two-point system. Both measurement volumes measure the u component. The two channels acquire the velocity samples independently (free-running mode) without coincidence.
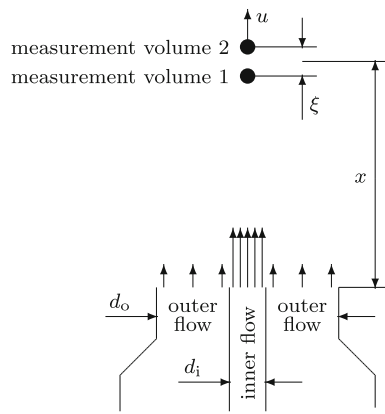
Fig. 1 Experimental setup

Table 1 Flow specifications

Outer diameter, d_o	140 mm
Inner diameter, d_i	8 mm
Outer velocity (at nozzle exit)	0.5 m/s
Inner velocity (at nozzle exit), U_0	35.9 m/s
Outer volume flux	27.6 m³/h
Inner volume flux	6.5 m³/h
Kinematic viscosity, v	14×10^{-6} m²/s (air)
Reynolds number, $\text{Re} = \frac{U_0 d_i}{v}$	2×10^4

Table 2 Specification of the laser Doppler system

Laser	Ar^+, max. 5 W used with 500 mW, multi-mode
Wavelength	514.5 and 488 nm
Optical configuration	Fiber-coupled probe, backscatter
Frequency shift	Bragg cell, 40 MHz
Focal length	310 mm
Measurement volume	400 μm × 50 μm
Processor	IFA750

The Reynolds number is 20,000 based on the inner mean velocity and diameter. The laser Doppler data have been taken in the center of the jet at a distance $x = 320$ mm ($40d_i$) downstream. The separation of the measurement volumes has been varied between $\xi = 0$ and $\xi = 32$ mm ($4d_i$) with symmetrical shifts of $\pm\xi/2$ with respect to x. For one-point measurements, the appropriate data sets have been selected from the two-point measurements.

The mean velocity U and the RMS velocity u' are obtained from the measurements as ensemble averages applying transit time weighting (Hösel and Rodi 1977; Fuchs et al. 1994). The mean velocity decays from 7.85 to 7.15 m/s over the measurement region, while the RMS velocity decays from 1.44 to 1.40 m/s. This corresponds approximately to an inverse relation with the distance to some virtual origin lying within the nozzle; the virtual origin of the RMS data being slightly further inside the nozzle than the mean velocity data set. A turbulence intensity u'/U of about 19 % is found, slightly increasing with the distance from the nozzle. Comparing with Wygnanski and Fiedler (1969), this small value indicates that the present free jet may not be fully developed in the measurement region; this is of no direct consequence for the present study.

The correlation functions are obtained from the measurements using the fuzzy slotting technique with local time estimation (Nobach 2002) and transit time weighting. Then, the correlation functions $R(\xi, \tau)$ have been normalized, yielding the correlation coefficient functions $\rho(\xi, \tau)$ with

$$\rho(\xi, \tau) = \frac{R(\xi, \tau)}{(u')^2} \tag{7}$$

using the RMS u' of the fluctuating part of the velocity for the autocorrelation cases and

$$\rho(\xi, \tau) = \frac{R(\xi, \tau)}{u'_1 u'_2} \tag{8}$$

for the cross-correlation cases, where u'_1 and u'_2 are the RMS velocities at the two measurement points.

Figure 2 shows the autocorrelation coefficient function obtained from the one-point experimental data. Note, that the variance estimates are biased by data noise, whereas the correlations are not, yielding an autocorrelation coefficient $\rho < 1$ at $\tau = 0$. Figure 3 shows examples of cross-correlation coefficient functions obtained from two sets of two-point experimental data for separations ξ of 0 and 32 mm. The two LDV measurement volumes for two-point
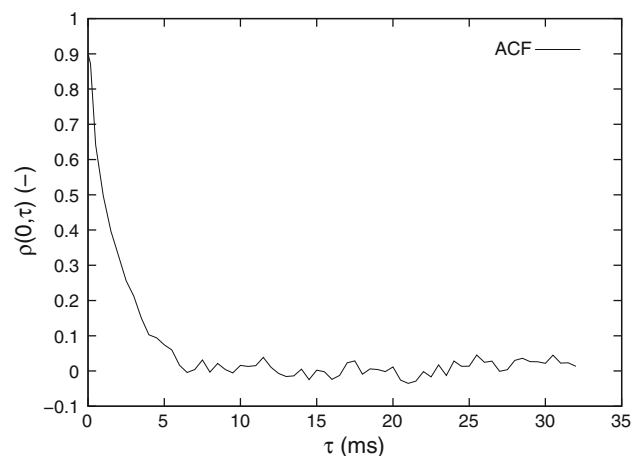

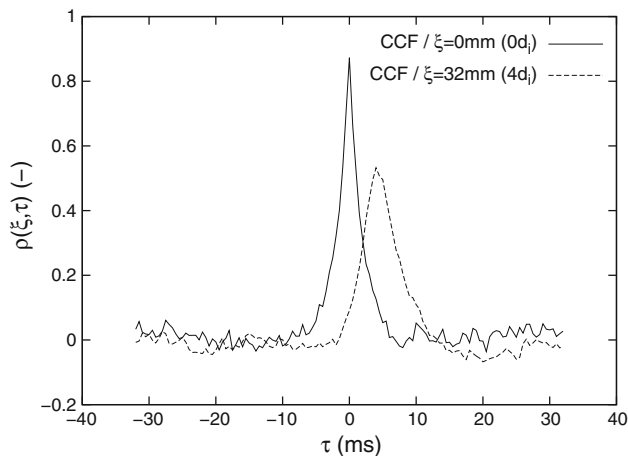**Fig. 2** Temporal autocorrelation function (ACF) obtained from one-point measurement

Fig. 3 Temporal cross-correlation functions (CCF) obtained from two-point measurements

Fig. 4 Comparison of the longitudinal spatial correlation functions obtained from one-point measurements using Taylor's hypothesis (TH) and the integral time-to-length transform (ITLT) compared to corresponding two-point measurements (CCF)

Fig. 5 Spatio-temporal correlation functions obtained from one-point measurements using Taylor's hypothesis (TH) and the integral time-to-length transform (ITLT) compared to corresponding two-point measurement (CCF) for a separation of $\xi = 32$ mm ($4d_i$) with the autocorrelation function (ACF) for comparison

measurements are aligned parallel. Therefore, the cross-correlation for two overlapping measurement points ($\xi = 0$) almost reaches the amplitude of the autocorrelation for one measurement point. While both the noise in the autocorrelation/one-point case and the differences between the measurement channels in the cross-correlation/two-point case generate systematic errors of the estimated correlation coefficients, this bias does not affect the following derivations of the spatio-temporal transform. Therefore, no corrections of the correlation functions have been undertaken.

Based on the mean velocity U and the RMS velocity u' obtained from the measured data set, the temporal correlation function is transformed into the longitudinal spatial correlation function using TH [Eqs. (1), (3)] and ITLT [Eqs. (5), (6)]. In the present study, a Gaussian distribution of the velocity u is assumed to derive the probability density function of times of flight. Alternatively, the probability density can be derived directly from the measured data.

Figure 4 shows the results of the two transforms in comparison with the longitudinal spatial correlation function obtained from two-point measurements. The results of the different methods have no significant deviations from each other or from the two-point cross-correlation. Even the simple transform based on TH shows reasonable results. This coincides directly with the results found in Tummers et al. (1995). For a flow with 25 % turbulence intensity, this is noteworthy, since this is far away from a "frozen" flow condition.

To understand this observation, a detailed look at the spatio-temporal correlation function is useful. Figure 5 shows the results of the transformation based on TH and ITLT in comparison with appropriate temporal cross-correlation functions from the two-point measurement at a separation of the
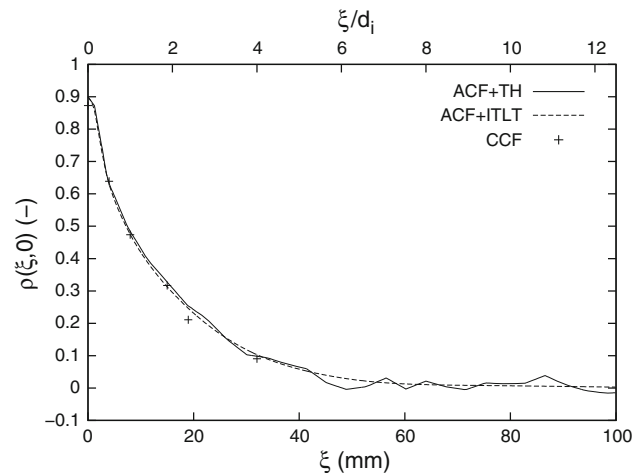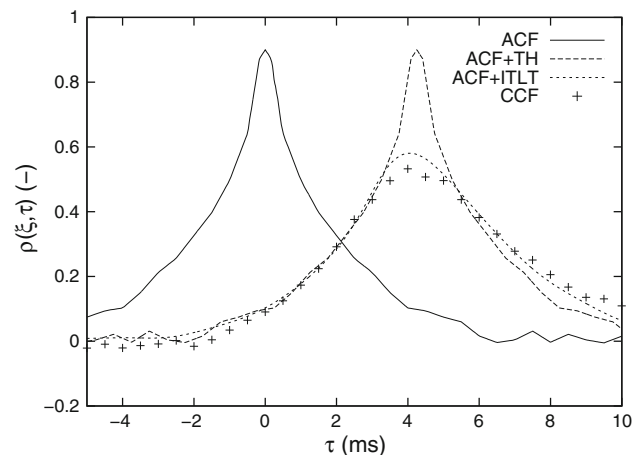
measurement volumes of $\xi = 32$ mm ($4d_i$). The shift in time of the maximum correlation corresponds to the mean time of flight to cover the separation. The height of the maximum decreases, which indicates that the shape of fluid structures changes during their passage. Furthermore, the peak width increases, indicating spatial diffusion of the fluid structures. Similar behavior has been shown by Kerhervé et al. (2008) for a turbulent round jet and by Cenedese et al. (1991) and by Chatellier and Fitzpatrick (2005) for other turbulent flow configurations.

TH simply shifts the autocorrelation function to the time of flight given by the separation of the probes divided by the mean velocity. The shape of the obtained spatio-
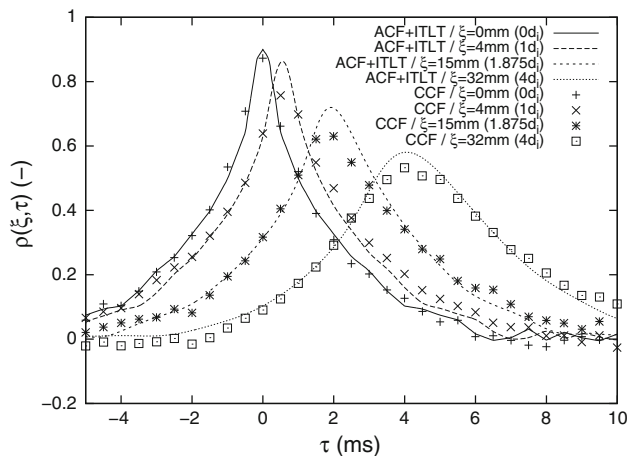
Fig. 6 Spatio-temporal correlation functions obtained from one-point measurements using the integral time-to-length transform (ITLT) compared to corresponding two-point measurements (CCF) at different separations ξ
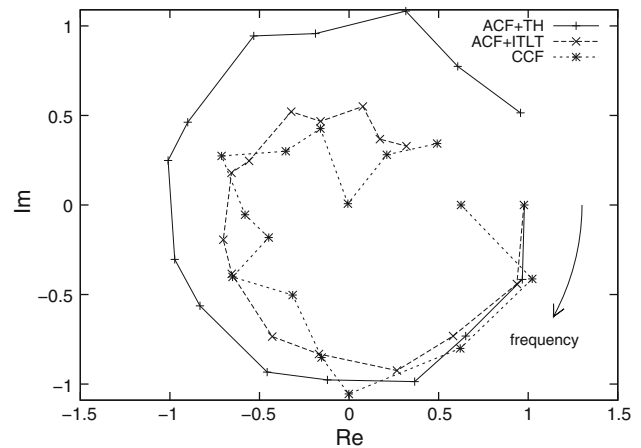

Fig. 7 Spectral transfer functions from the autocorrelation function to the spatio-temporal correlation from the experiment (CCF), Taylor's hypothesis (TH) and the integral time-to-length transform (ITLT) for a separation of $\xi = 32$ mm ($4d_i$)

temporal correlation function is the same as the autocorrelation function. Therefore, the transform based on TH is not able to reproduce the degradation of the correlation height or the expansion of the correlation width. However, the accuracy of the predicted time shift by TH is additionally limited due to the fact that the maximum position of the correlation peak may deviate from the separation divided by the mean velocity due to a skewness of the deformed peak. This yields a correlation peak traveling slower than the mean velocity as observed by He and Zhang (2006) and in Zhao and He (2009).

In contrast, ITLT is able to recover the spatio-temporal correlation correctly, including the time shift, the degradation of the correlation height and the expansion of the correlation width. Even the skewness of the peak is reproduced correctly.

In Fig. 6, the results of ITLT are shown in comparison with the two-point measurements for different longitudinal spatial separations of the two measurement volumes. The results of ITLT clearly correspond to the two-point measurements, indicating that ITLT is an appropriate model for the temporal development of fluid structures, while the result for TH would fail.

Although the spectral transfer functions from the autocorrelation to the modeled spatio-temporal correlation functions are redundant, if the time responses are correct, it is still interesting to verify the correspondence of the obtained transfer functions with the results in Cenedese et al. (1991). Therefore, the experimentally obtained spatio-temporal correlation functions and the pendents obtained by TH and ITLT are Fourier transformed and divided by the Fourier transform of the autocorrelation function.

The diagrams in Fig. 7 show the first 15 complex spectral transfer coefficients for the case $\xi = 32$ mm ($4d_i$).

The result of TH rotates in the complex plane with unit magnitude, corresponding to a simple time shift. Although the experimental data strongly scatter, ITLT obviously reproduces the amplitude decreasing with increasing frequency, yielding similar results as in Cenedese et al. (1991).

Unfortunately, if u changes within the separation ξ (or within the time of flight θ) the probability density function of times of flight changes and also the fluid structure passing by changes, yielding an additional degradation of the correlation. This case is a strong limitation of the present transformation method, which requires the temporal correlation in the Lagrangian framework to be much longer than the time of flight for a certain velocity and a given separation of the measurement volumes.

An indication on how good this requirement is fulfilled is given by comparing the integral time scales derived as the integral of the cross-correlation coefficient functions for different separations of the measurement volumes. If the requirement of small changes during the passage is fulfilled, the integral time scale should be constant and independent of the separation of the measurement volumes. Figure 8 shows the integral time scales obtained from the two-point measurements. With increasing separation, a small decrease in the integral time scale can be observed. However, it is small enough to allow reliable application of the ITLT method.

4 Longitudinal spatial correlation

In deriving the spatio-temporal correlation function, ITLT is clearly superior to the TH. However, if only the longitudinal spatial correlation function is required at turbulence levels at least up to 25 %, the TH performs as well (Fig. 4).
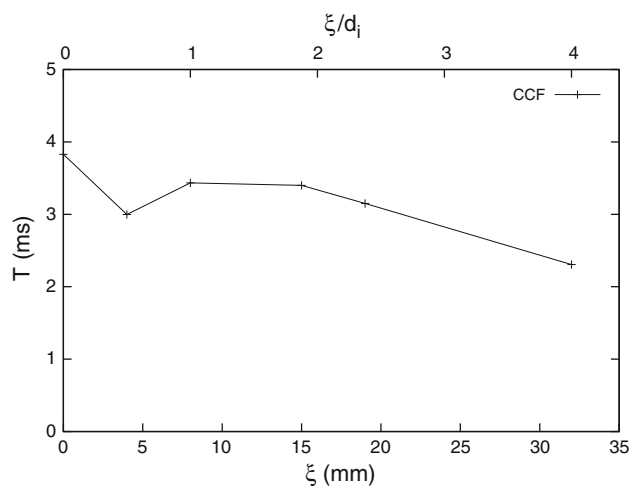
Fig. 8 Integral time scales obtained from the cross-correlation function of experimental two-point measurements as a function of the separation of the measurement volumes

To estimate the longitudinal spatial correlation function from two-point measurements, only the values at $\tau = 0$ (coincidence) are measured for several separations ξ, while all other time lags of the spatio-temporal correlation are not taken into account. However, on the left tail of the spatio-temporal correlation function, the two transform methods almost coincide (Fig. 5). Significant deviations are visible only at the peak center and on the right tail of the spatio-temporal correlation function. Only for turbulence levels above at least 25 % could we expect deviations on the left tail of the spatio-temporal correlation functions occurring between the TH and ITLT, yielding also differences between the longitudinal spatial correlation functions.

5 Conclusion

An integral time-to-length transform method has been introduced. It is capable of reproducing the longitudinal spatial-temporal correlation by considering fluctuations of the varying convective velocity. Therefore, it is able to provide longitudinal spatial and spatio-temporal correlation functions from temporal correlation functions obtained from single-point measurements. In the case of turbulent flows, it is superior to Taylor's hypothesis of a "frozen" flow. The integral transform method is able to recover the spatio-temporal correlation correctly, including the time shift, the degradation of the correlation height, the expansion of the correlation width and the skewness of the peak.

On the contrary, the transform of a temporal correlation function into a longitudinal spatial correlation function based on Taylor's hypothesis is possible up to turbulence intensities of at least 25 %, because the systematic errors

are small, even if the model of a "frozen" flow is far from reality. However, for turbulence intensities beyond 25 %, differences between the methods may occur also at the time lag $\tau = 0$; hence, differences of the obtained longitudinal spatial correlation function must be expected as well. However, Taylor's hypothesis is not able to recover the temporal development of fluid structures and, therefore, is not capable of transforming temporal correlation functions into spatio-temporal correlations, which the integral method is able to reproduce reliably.

References

Browne LWB, Antonia RA, Rajagopalan S (1983) The spatial derivative of temperature in a turbulent flow and Taylor's hypothesis. Phys Fluids 26:1222–1227

Cenedese A, Romano GP, Di Felice F (1991) Experimental testing of Taylor's hypothesis by L. D. A. in highly turbulent flow. Exp Fluids 11:351–358

Chatellier L, Fitzpatrick J (2005) Spatio-temporal correlation analysis of turbulent flows using global and single-point measurements. Exp Fluids 38:563–575

Cholemari MR, Arakeri JH (2006) A model relating Eulerian spatial and temporal velocity correlations. J Fluid Mech 551:19–29

Favre AJ (1965) Review on space-time correlations in turbulent fluids. Trans ASME J Appl Mech 32:241–257

Fuchs W, Nobach H, Tropea C (1994) Laser Doppler anemometry data simulation: application to investigate the accuracy of statistical estimators. AIAA J 32:1883–1889

He GW, Zhang JB (2006) Elliptic model for space-time correlations in turbulent shear flows. Phys Rev E 73:055303(R)

Heskestad G (1965) A generalized Taylor hypothesis with application for high Reynolds number turbulent shear flows. J Appl Mech 87:735–739

Hill RJ (1996) Corrections of Taylor's frozen turbulence approximation. Atmos Res 40:153–175

Hösel W, Rodi W (1977) New biasing elimination method for laser-Doppler-velocimeter counter processing. Rev Sci Instrum 48:910–919

Kerhervé F, Fitzpatrick J, Chatellier L (2008) A sensitivity analysis of the point reference global correlation (PRGC) technique for spatio-temporal correlations in turbulent flows. Exp Fluids 44:577–589

Lin CC (1953) On Taylor's hypothesis and the acceleration terms in Navier-Stokes equations. Q Appl Math 10:295–306

Nobach H (2002) Local time estimation for the slotted correlation function of randomly sampled LDA data. Exp Fluids 32:337–345

Ouellette NT, Xu H, Bodenschatz E (2006) A quantitative study of three-dimensional Lagrangian particle tracking algorithms. Exp Fluids 40:301–313

Romano GP, Antonia RA, Zhou T (1999) Evaluation of LDA temporal and spatial velocity structure functions in a low Reynolds number turbulent channel flow. Exp Fluids 27:368–377

Taylor GI (1938) The spectrum of turbulence. Proc R Soc Lond Ser A 164:476–490

Tennekes H (1975) Eulerian and Lagrangian time microscales in isotropic turbulence. J Fluid Mech 67:561–567

Tummers MJ, Passchier DM, Aswatha Narayana PA (1995) LDA measurements of time- and spatial correlation functions in an adverse pressure gradient wake. In: Proceedings ASME/JSME Fluids Engineering and Laser Anemometry Conference Hilton Head Island, South Carolina, USA, pp 347–355. FED-Vol 229

Wygnanski I, Fiedler H (1969) Some measurements in the self-preserving jet. J Fluid Mech 38:577–612

Zhao X, He GW (2009) Space-time correlations of fluctuating velocities in turbulent shear flows. Phys Rev E 79:046316